RSC Advances

ROYAL SOCIETY OF CHEMISTRY

www.rsc.org/advances

Graphical abstract

Graphical abstract: In view of dewatering bottleneck of resource utilization of sewage sludge, we proposed a strategy that integrates wet sludge treatment with catalyst preparation and heavy metals in catalysts have been solidified in catalyst to prevent their leaching to solution.

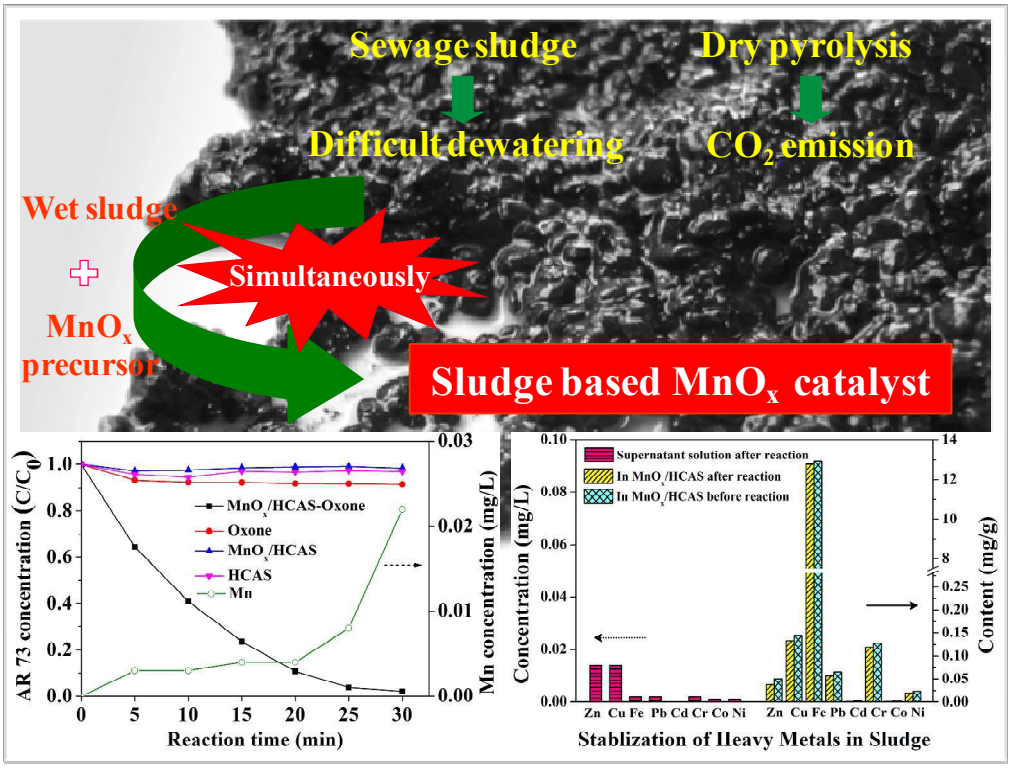

Fabrication of MnO_x heterogeneous catalyst from wet sludge for degradation of azo dyes by activated peroxymonosulfate

Lili Xu[a], Wanpeng Liu[a], Xingfa Li[a], Sadia Rashid[b], Chensi Shen[b], Yuezhong Wen[a*,c]

[a]Institute of Environmental Science, Zhejiang University, Hangzhou 310058, China

[b]College of Environmental Science and Engineering, Donghua University, Shanghai 201620, China

[c]Zhejiang Provincial Key Laboratory of Organic Pollution Process and Control, Zhejiang University, Hangzhou 310058, China

* Corresponding author:

Tel.: +86-571-8898-2421. Fax: +86-571-8898-2421.

E-mail address: wenyuezhong@zju.edu.cn (Y.W.)

ABSTRACT

For dewatering and resource utilization of sewage sludge, catalyst preparation paralleled with sewage sludge dewatering, was explored. In order to obtain a better understanding of this strategy, anaerobic sludge based MnO_x catalyst (MnO_x/HCAS) was characterized, and tested in activation of Oxone for dye degradation in aqueous solution. The multi-valence oxidation states of manganese were formed in MnO_x/HCAS. The catalyst exhibits high catalytic activity towards Oxone for the degradation of dyes in aqueous solution. The kinetic data followed first order kinetics with the activation energy of 21.87 kJ/mol. The evaluation of the reusability of MnO_x/HCAS showed that MnO_x/HCAS exhibited high stability in recycled tests without losing its activity. The removal of a variety of anionic dyes also demonstrates an excellent catalytic performance of MnO_x/HCAS. To investigate stabilization of heavy metals in the catalyst, leaching test was conducted, and the result showed that heavy metals can be solidified to prevent their leaching to solution. The effect of different kinds of wet sludge was investigated. And all these sludges based MnO_x catalysts exhibit good catalytic performance to azo dyes with degradation rates more than 98%, which decides its unquestionable possibility for fabrication of MnO_x heterogeneous catalyst from wet sludge and its practical applications.

Keywords: wet sludge; resource utilization; MnO_x catalyst; hydrothermal process; azo dyes

1. Introduction

Currently wastewater treatment sludge (WWTS) is one among the waste biomass produced in abundant quantity with high water content (up to about 98 wt%)[1], making the disposal of WWTS a pressing environmental problem. The traditional disposal alternatives for sewage sludge include landfill, composting, land application following aerobic and anaerobic digestion, and incineration, none of which are exempt from the risk of contaminating the environment, and threatening human health[2-4]. And the associated regulations are also becoming stricter[5,6]. Converting waste into useful products can alleviate the disposal problems and offer a new reserve for depleting resources[7-10]. As an alternative, the hydrothermal treatment technology (HTT) was developed to harness energy from wet sewage sludge to avoid high-energy prior to drying. In previous studies on HTT of wet sewage sludge, hydrothermal liquefaction (HTL) was applied for the production of crude bio-oil at elevated temperature (250-380 ºC) and pressure (10-25 MPa)[11], as well as the production of hydrogen (H_2) and methane (CH_4) through hydrothermal gasification[12]. However, high reaction temperature means high cost and will bring severe operational issues such as corrosion and scaling[13]. Thus, the interests of recent studies have focused on hydrothermal carbonization (HTC). An important technique for the production of various carbonaceous materials and hybrids, usually applied at mild temperatures (≤ 200 ºC), and in pure water inside closed recipients and under self generated pressure. There is no drying in HTC because water serves as the reaction medium. Therefore, wet sludge is suitable for HTC. Furthermore, there are some other advantages in HTC:

(1) the reaction temperature of HTC is usually much lower than other carbonization methods, such as pyrolysis or hydrothermal gasification and (2) HTC can reduce greenhouse gas emission, as only a small amount of gas, particularly CO_2, is generated[14].

In the meantime, it should be noticed that hydrothermal method also has been applied for the preparation of many catalysts with excellent catalytic activities. For example, Yao et al. proposed a facile approach for preparing Co_3O_4-reduced graphene oxide via hydrothermal synthesis under basic conditions and applied it for the decomposition of phenol[15]. However, Co^{2+} is highly toxic and can cause some health problems. Thus, attempts to use less toxic Mn oxides have been reported recently. MnO_2 is also widely used in heterogeneous catalysis due to its physical and chemical properties[16-18]. Capitalizing this fact, we conjectured that it might be possible to develop a strategy that integrates wet sludge treatment with catalyst preparation by hydrothermal carbonization. To the best of our knowledge, no such work has been reported before. Since sewage sludge is a complex mixture of various components containing carbohydrates, humic substances, heavy metals and so on. Therefore, in order to obtain a better understanding of this strategy, the following questions need be answered: (1) it is not clear whether the combination of wet sludge treatment and catalyst preparation by hydrothermal process is feasible; (2) how about the efficiency and stability of such prepared catalysts and (3) can we stabilize and solidify these toxic heavy metals in catalysts in order to prevent their leaching?

To decipher the puzzle, we synthesized an effective MnO_x heterogeneous

catalyst from wet sludge via hydrothermal carbonization under mild conditions (120 ºC or 200 ºC) and the prepared catalysts were used for the catalytic degradation of azo dyes by activated peroxymonosulfate (Oxone). As we know, wastewater discharged from dyeing processes is one of the biggest contributors to textile effluent; this comprises mainly residual dyes and auxiliary chemicals[19,20]. Among these dyes, azo dyes represent the largest class of dyes[21,22]. In the meantime, sulfate radicals initiators such as Oxone have been explored due to their high oxidation power[23].

2. Materials and methods

2.1. Materials

$MnSO_4 \cdot H_2O$ and $(NH_4)_2S_2O_8$ were obtained from National Medicines Co., Ltd, Shanghai, China. Peroxymonosulfate (Oxone, $2KHSO_5 \cdot KHSO_4 \cdot K_2SO_4$) was purchased from Sigma-Aldrich. C. I. Acid Red 73 (AR 73) and other dyes were obtained from Gracia Chemical Technology Co., Ltd. (Chengdu, China). The purities of dyes were over 99.5% (chemical structures are shown in Figure S1 in Supporting Information). The anaerobic sludge (AS) was obtained from the Qi-ge wastewater treatment plant, Hangzhou, China (the physicochemical characteristics of anaerobic sludge are presented in Table S1 in Supporting Information). Other types of sludge from different wastewater treatment plant, including primary, secondary and digested sewage, were chosen in this study. The high-purity water used in this study was produced using a UPK/UPT ultrapure water system. Other chemical reagents were of analytical grade and used without any further purification.

2.2. Fabrication of MnO_x heterogeneous catalyst from wet sludge

The MnO_x/HCAS catalyst was prepared by one-pot hydrothermal synthesis in a laboratory-scale stainless-steel autoclave (GSH-0.5L, Shandong, China) equipped with an electric stirrer (Figure S2). The stainless-steel container was filled with a volume of 0.2 L anaerobic sludge (water content: 80.01%), subsequently, 0.020 M $MnSO_4 \cdot H_2O$ was added progressively to the reactor with vigorous stirring at room temperature to obtain a well-mixed solution, and left to stand for 12 h. Then, 0.024 M $(NH_4)_2S_2O_8$ was placed into the autoclave with stirring and maintained at 120 ºC and 200 ºC for 12 h, which were regulated by a programmable controller. The target temperature and the reaction duration were set in the control panel. The resulting product was centrifuged, decanted, washed with deionized water and dried at 80 °C in air. In addition, other types of sludge based MnO_x catalysts were prepared under the same conditions stated above.

To investigate the combine effect of sludge treatment and catalyst preparations, two possible approaches were examined. The first involved adding separate anaerobic sludge and $MnSO_4 \cdot H_2O$ into the stainless-steel container simultaneously, then treating them for 12 h at 120 ºC and 200 ºC, respectively (MnO_x/HCAS-120 and MnO_x/HCAS-200). And the second involved pretreating anaerobic sludge by HTC process at 200 ºC for 12 h and then adding $MnSO_4 \cdot H_2O$, finally treating them by HTC process at 120 ºC for 12 h (MnO_x/HCAS-200-120). Also two control experiments as mentioned above, HCAS-120 and HCAS-200 were conducted. The degradation studies (pH 7) were carried out in order to optimize the suitable preparation conditions for maximum catalytic activity, and the results were given in Table S2. It

can be seen that the adsorption experiments indicated that MnO_x/HCAS or HCAS materials had less adsorption for AR 73 (<3%). In method 1, the degradation rate of AR 73 by MnO_x/HCAS-120 with Oxone was 98.3% after 30 min, much higher than the MnO_x/HCAS-200 catalyst (10.2%). Also, in method 2, the MnO_x/HCAS-200-120 showed high degradation of AR 73 (98% after 30 min). These results suggested that the temperature of catalyst preparation is more important than the support for combination of sludge treatment and MnO_x catalyst. To obtain a high catalytic activity of the catalyst, low preparation temperature should be controlled since low preparation temperature means low energy consumption. Therefore, the combination of sewage sludge treatment with catalyst preparation is feasible. In comparison with MnO_x/HCAS-200-120, the preparation process of MnO_x/HCAS-120 was more convenient. Thus, MnO_x/HCAS-120 was chosen as the optimal catalyst in this study.

The MnO_x/HCAS was characterized by X-ray diffraction (XRD), scanning electron microscopy (SEM), X-ray absorption near-edge spectroscopy (XANES) and Soft X-ray scanning transmission X-ray microscopy (STXM). The details are described in Text S1 in Supporting Information. Nitrogen adsorption and desorption isotherms at 77 K were measured using NOVA2000e surface area & pore size analyzer (Quantachrome, USA). The specific surface area was calculated by Brunauer-Emmet-Teller (BET) equation.

2.3. Experimental procedures and analysis

To evaluate the activity of catalytic oxidation of dye, batch experiments were carried out in 250 mL conical flasks at 25 ºC with constant stirring at 150 rpm. A

desired amount of Oxone was added to the dye solution (100 mL). Solution pH was adjusted by H_2SO_4 or NaOH. Then the reaction was initiated once the catalyst was added. At predetermined time internals, aqueous phase samples (2.5 mL) were withdrawn and immediately filtered (0.22 μm) to remove the catalyst solids. Subsequently, the concentrations of remnant dye were analyzed using a Shimadzu UV-2401PC UV-Vis spectrometer (Tokyo, Japan) at its absorbance maximum.

The mineralization of dye solution was determined by measuring the decrease of chemical oxygen demand (COD) of the supernatant solution. The supernatant solution was refluxed with potassium dichromate in the presence of silver and mercury sulfate at 100 ºC for 2 h. The refluxed solution was then titrated with ferrous ammonium sulfate (FAS) using ferroin as an indicator. Similar conditions were used for the blank sample (distilled water). COD was calculated by using the formula: COD (mg L^{-1})=$(A-B)\times N\times 8\times 1000/C$, where A is the volume of FAS required for the blank (mL), B is the volume of FAS required for the effluent sample (mL), N is the normality of FAS, and 8 is the milliequivalent weight of oxygen and$C$ is the volume of supernatant solution or distilled water (mL).

For the stability test of the catalyst, the used catalyst was collected by centrifugation, washed with deionized water and dried at 80 ºC in air. Catalyst dose and other reaction conditions remained the same for the subsequent runs. Furthermore, inductively coupled plasma mass spectrometry (ICP-MS) elemental analysis was performed in the present study. The leaching test was conducted with 50 mg/L of dye solution prepared at a liquid-solid ratio of 100 mL/0.1 g (pH 7.0±0.2) and stirred at

150 rpm for 30 min. After centrifugation, the supernatant solution was analyzed using flow injection coupled with ICP-MS (ELAN DRC-e ICP-MS from Perkin-Elmer company).The total contents of heavy metals in MnO_x/HCAS catalyst before and after reaction were extracted by acid digestion (using HNO_3/$HClO_4$/HF) and then were examined by ICP-MS.

3. Results and discussion

3.1. Characterization of Catalyst

The chemical property of AS, HCAS-120, and HCAS-200 was studied. The changes in the major elemental composition (C, H, O and N) of AS, HCAS-120 and HCAS-200 were quantified and the results were listed in Table 1. It can be seen that the C content decreased with the increasing reaction temperature as a result of oxygenating reactions (AS:14.75%, HCAS-120:13.56%, and HCAS-200:9.02%), which were particularly evident at 200 ^{o}C. This is because the polysaccharide decomposed into CO_2 and water at the temperature above 180 ^{o}C[24]. At the same time, H and O contents also decreased due to dehydration and decarboxylation reactions during HTC processes. Besides, H/C and O/C ratios declined with the rise of the temperature, indicating an increasing degree of carbonization of AS.

The prepared samples were first characterized by XRD to identify its crystallographic structure. The XRD patterns of HCAS (a), pure MnO_2 (b) and MnO_x/HCAS (c) are shown in Figure S3. The XRD pattern of HCAS reveals the presence of important amount of quartz, and the peak at 2θ=26.3 º can be attributed to the diffraction of the (002) plane of the disordered carbon structure, due to the

carbonization of anaerobic sludge. The characteristic peaks of carbon structure were also observed in the XRD pattern of MnO_x/HCAS. Additionally, no significant signals corresponding to pure MnO_2 phase (JCPDS No. 72-1982)[25] in the XRD pattern of MnO_x/HCAS were observed. This may be attributed to the small MnO_2 crystalline size or the presence of an amorphous MnO_2 phase deposited onto the HCAS, as previously reported[26-28]. According to the results of BET surface area, HCAS presented the highest BET surface area (55.469 m^2/g), whereas MnO_x/HCAS presented the lowest surface area (37.402 m^2/g). The BET surface area of MnO_x/HCAS decreased because of the in situ synthesis of MnO_x nano-particles into the HCAS.

The morphology and structure of HCAS and MnO_x/HCAS were further examined with SEM. As shown in Figure 1a and 1b, the HCAS particles were irregular and in a relatively agglomerated state in the range of micrometers. This may be caused by extracellular polymeric substances (EPS), which exists in flocs and cellular tissues of anaerobic sludge[29]. When simultaneous wet sludge treatment and MnO_x catalyst preparation were conducted, it can be observed that the shape of the MnO_x/HCAS particles (Figure 1c and 1d) is also irregular, but the agglomeration is relieved, because the in situ synthesis of MnO_x onto HCAS, to some extent may hinder EPS agglomeration into larger particles by binding onto HCAS.

In addition, the valence state of manganese in MnO_x/HCAS catalyst was determined from XANES. Figure 2 shows the normalized Mn K-edge XANES spectra of the MnO_x/HCAS sample with a series of reference compounds such as pure Mn metal, MnO, Mn_3O_4, Mn_2O_3 and MnO_2. It can be observed that the position of manganese absorption edge shifts with the increase of the oxidation state of Mn atoms.

For MnO_x/HCAS catalyst, the Mn K-edge XANES data exhibit edge shifts in the region between the Mn K-edges of Mn_2O_3 and MnO_2 reference compounds, indicating that the average oxidation states of manganese in MnO_x/HCAS sample must be between 3+ and 4+[30].

3.2. Catalytic performance

The experiments were performed in different processes to investigate the degradation efficiency of AR 73, including Oxone alone, MnO_x/Oxone, and MnO_x/HCAS/Oxone. Also the control experiments were investigated to determine the adsorption abilities of MnO_x, MnO_x/HCAS and HCAS. As shown in Figure 3, for Oxone alone, dye degradation showed a minor change and was less than 8% after 30 min, suggesting that Oxone itself fails to induce oxidation degradation of the dye. In the absence of Oxone, the catalysts MnO_x, MnO_x/HCAS and HCAS also presented low adsorption efficiencies with only 2-6% removal. However, with the co-existence of Oxone and MnO_x or MnO_x/HCAS, AR 73 concentration decreased significantly and the degradation rate reached over 98%. However, nano-MnO_x is very difficult to be separated from water, and this becomes the major limitation for the application of nano-materials in the field of wastewater treatment. In addition, other anionic dyes were also effectively degraded by MnO_x/HCAS/Oxone (Table 2). The catalytic oxidation of dyes would be due to the synergistic effect of MnO_x/HCAS and Oxone. MnO_x/HCAS can induce the decomposition of Oxone and produce sulfate radicals as shown in the following equations.

$$HSO_5^- + MnO_2/HCAS \longrightarrow SO_5^{-\bullet} + OH^- + Mn_2O_3/HCAS \qquad (1)$$

$$HSO_5^- + Mn_2O_3/HCAS \longrightarrow SO_4^{-\bullet} + H^+ + MnO_2/HCAS \quad (2)$$

$$SO_4^{-\bullet} + H_2O \longrightarrow HO^\bullet + H^+ + SO_4^{2-} \quad (3)$$

$$AR\ 73\ (C_{22}H_{14}N_4Na_2O_7S_2) + SO_4^{-\bullet} \longrightarrow AR\ 73\text{-}SO_4^{-\bullet}$$

$$\longrightarrow \text{several steps}$$

$$\longrightarrow CO_2 + H_2O + N_2 + SO_4^{2-} \quad (4)$$

To identify the dominating radical species in MnO_x/HCAS/Oxone system, quenching studies were performed. $SO_5^{-\bullet}$ radical would not contribute to dye degradation because of its lower redox potential. Therefore, Methanol (MeOH) and tert-butyl alcohol (TBA) were selected as quenching agents since MeOH is widely used as the scavenger of $SO_4^{-\bullet}$ and $HO^\bullet$ while TBA is the effective quenching agent for $HO^\bullet$[31]. In the absence of quenching agents, dye degradation was very fast and reached 98% in 30 min. However, as shown in Figure S4, MeOH and TBA indeed inhibited the dye degradation. It can be seen that the degradation rates were 42% and 78% in the presence of MeOH (0.3 mol/L) and TBA (0.3 mol/L) in 30 min, respectively. In comparison to the decrease in dye degradation rate in the presence of TBA, relatively significant decrease in the presence of MeOH indicated that $SO_4^{-\bullet}$ as radical species were predominantly produced during the decomposition of Oxone by MnO_x/HCAS. The results justified the involvements of both $SO_4^{-\bullet}$ and $HO^\bullet$ radical mechanism in the MnO_x/HCAS/Oxone system.

3.3. Effects of inorganic salts and reaction temperature

In general, a great amount of inorganic salts are employed in various dyeing processes and the strength of dissolved inorganic ions in dyestuff wastewater may

affect the efficiency of dye degradation reaction[32]. However, there is usually a large salinity range[33, 34]. In this study, the influences of two common inorganic salts at the range of 1-150 mg/L (NaCl and $NaHCO_3$) on the catalytic degradation of dye solutions were assessed and the experimental results are presented in Figure 4a and 4b, respectively. It can be obviously seen that NaCl had a positive effect on dye degradation and the progressive increase in degradation was identified with the increasing concentration of NaCl solution from 1 to 150 mg/L by comparing with control (without inorganic salts). Wang et al. reported a xanthene dye Rhodamine B degradation in Fe(II)/Oxone system and found that in the presence of Cl^- can significantly improve dye degradation[35], which is similar to the observation in this study. It is known that Cl^- can be oxidized by $SO_4^{-\bullet}$ to form chlorine radicals, which may result in a series of secondary oxidants, such as $Cl^\bullet$, $Cl_2^{-\bullet}$ and HOCl. These secondary oxidants were likely to enhance the dye degradation, involving the reaction of chlorine radicals and free available chlorine species. However, for MnO_x/HCAS/Oxone system at a lower concentration (1 mg/L), the $NaHCO_3$ showed a negligible effect on dye degradation. But above 1 mg/L, $NaHCO_3$ showed negative influences on dye degradation (Figure 4b). The degradation rate of AR 73 gradually decreased from 91% to 72% after 30 min, as the dosage of $NaHCO_3$ increased from 10 to 150 mg/L. One possible explanation was that the $NaHCO_3$ would mostly act as $HO^\bullet$ and $SO_4^{-\bullet}$ scavengers at high concentrations (>10 mg/L) and therefore inhibit dye degradation[36].

The effect of temperature (15, 25, 35 and 45 ºC) on dye degradation was also

investigated. It can be seen from Figure 4c that increasing temperature had a positive effect on AR 73 degradation for the MnO_x/HCAS catalyst. The results showed that increasing the reaction temperature from 15 to 45 ºC enhanced the AR 73 degradation efficiency from 64 to 94% in 15 min. This is due to the fast Oxone decomposition at high temperatures, which in turn generates more active radicals than that at low temperatures. Based on the first order kinetics, the reaction rate constants were determined and the dependence of rate constants on the temperature obeyed the Arrhenius relationship with R^2=0.9968 as shown in the inset of Figure 4c. The activation energy (*Ea*) for the degradation process was calculated to be 21.87 kJ/mol. For Oxone activation by heterogeneous MnO_x/HCAS catalyst in dye degradation, few investigations have been reported on the kinetics and activation energies. However, previous investigations showed that the activation energy of reactions on different heterogeneous catalysts is between 49.01-69.23 kJ/mol, such as 49.01 kJ/mol on $Co_xFe_{3-x}O_4$-Rhodamine B, 49.50 kJ/mol on Co-graphene hybrid-Orange II and 69.23 kJ/mol on porous Fe_2O_3-Rhodamine B[37-39]. Even though it is unlikely for a comparison of the catalytic activity among various heterogeneous catalysts because of the difference in experimental conditions, the results suggest that MnO_x/HCAS catalyst will be a promising catalytic material for oxidation processes.

3.4. Stability of MnO_x/HCAS

In general, the most important aspect for catalyst is its efficiency and stability[40]. Owing to the high activity of MnO_x/HCAS catalyst in activation of Oxone for the generation of active radicals and the subsequent degradation of AR73, it is essential to

evaluate the reusability of the spent catalyst. As shown in Figure 5a, MnO_x/HCAS catalyst showed high catalytic performance during five recycling runs, with dye degradation efficiencies more than 98% and COD removal efficiencies varied from 43.5% to 45.0%.

In addition, because of the physical-chemical processes that are involved in activated wastewater sludge treatment, sludge tends to accumulate heavy metals existing in the wastewater. Stabilization and solidification of heavy metals in catalysts must be considered to prevent heavy metals leaching into solution during wastewater treatment. To investigate whether it is safe to use HCAS as support for MnO_x, ICP-MS elemental analysis was performed. It can be seen from Figure 5b that the concentration of heavy metals from the supernatant solution after reaction was very low, except for Zn and Cu. The leaching concentration of both Zn and Cu in supernatant solution was 0.014 mg/L, which is far less than the limits reported in drinking water by US Environmental Protection Agency[41]. Besides, there is no dramatic change for the contents of the heavy metals in MnO_x/HCAS catalyst after the reaction. To further investigate the stability of heavy metals in catalysts, based on a dual-energy ratio-contrast image method, the spatial distributions of above mentioned heavy metals, except Pb (Pb was not allowed to be determined), Cd and Co (the contents were too low), were depicted with soft X-ray scanning transmission X-ray microscopy (STXM) images at different energies (Detailed procedure is presented in the SI Text S1 and NEXAFS spectra of Fe, Ni, Zn, Cu and Cr reference at the L-edge are shown in the SI Figure S5). Figure 6 shows the STXM analysis of

element distribution of Fe, Ni, Zn, Cu and Cr in the MnO_x/HCAS catalyst before reaction and after five recycling runs. The distributions of these heavy metals were basically unchanged though the MnO_x/HCAS catalyst was reused up to 5 cycles. It is, therefore, concluded from the above results that heavy metals can be solidified in the MnO_x/HCAS catalyst, which pose no harmful impact on the environment.

3.5. Effect of different kinds of wet sludge

Sludge, originating from the treatment process of waste water, is the residue generated during the primary (physical and/or chemical), secondary (biological) and the tertiary (additional to secondary, often nutrient removal) treatment. There are three main categories of sludge: (1) sludge originating from the treatment of urban waste water, consisting of domestic waste water or in a mixture with industrial waste water and run-off from rain water, (2) sludge originating from the treatment of industrial waste water, and (3) sludge from drinking water treatment. The complicated structures of sludge may affect the preparation and performance of the catalysts. Therefore, in order to investigate the effect of different kinds of wet sludge on the catalyst preparation, aerobic and anaerobic sludge from different wastewater treatment plants, including primary, secondary and digested sewage, were chosen as catalyst supports in this study. As shown in Figure 7, all these sludge-based MnO_x catalysts exhibit excellent catalytic performances to azo dyes with degradation efficiencies more than 98% after 30 minutes of contact. Without adding Oxone, all these sludge-based MnO_x catalysts have low adsorption efficiencies with less than 30% removal, which also decided the possibility of practical applications for fabrication of

MnO_x heterogeneous catalyst from wet sludge.

3.6. Technical implications

Resource utilization of sewage sludge has recently received considerable attention. However, dewatering is a key bottleneck. Our experimental work confirmed the feasibility of combination of sewage sludge treatment with catalyst preparation and indicated this strategy as an attractive new alternative technology for sewage sludge treatment. It operates under mild conditions without dewatering wet sewage sludge and addition of high energy input (temperature: 120 ºC). The HTC reaction products were separated into water-soluble and water-insoluble parts. As well demonstrated in many previous studies on thermo-chemical conversion of biomass, the water-soluble products consist mainly of carbohydrates, acetic acids, aldehydes and pyran derivatives, all of which are oxygen-containing compounds[42,43]. However, more attention should be paid on the water-soluble fraction which can be easily separated by decanting. For future studies, the water-soluble organics will be analyzed and utilization of the liquid products will be investigated.

The variety of sewage sludge from different wastewater plants has complex characterization. Organic matter, heavy metals and microstructures in sewage sludge would have a significant impact on its resource utilization. Therefore, further studies are needed to explore the effects of these factors in detail. In addition, as we know, contaminants are harmful to human and environment, especially heavy metal contaminants [44-46]. Therefore, although our study suggested heavy metal's stability in sewage sludge, more toxicity test should be addressed in future for risk assessment.

4. Conclusion

A low-cost catalyst material, anaerobic sludge based MnO_x catalyst (MnO_x/HCAS) was characterized. This catalyst showed high efficiency in activation of Oxone for the generation of active radicals and the subsequent degradation of AR73. In the meantime, after the MnO_x/HCAS catalyst was reused in five runs, AR73 degradation efficiency can still be more than 98% and COD removal efficiencies varied from 43.5% to 45.0%. Furthermore, heavy metals in the catalyst had been solidified in the MnO_x/HCAS catalyst to prevent their leaching into solution and pose no harmful impact on the environment. In addition, different kinds of wet sludge based MnO_x catalysts also exhibit excellent catalytic performance to azo dye. Thus, this green, technically feasible, highly efficient and cost effective catalyst is very attractive and implies a potential for practical application for dye wastewater treatment.

Acknowledgments

The authors acknowledge financial support from 863 Research Project (2013AA065202), the Fundamental Research Funds for the Central Universities and Zhejiang University of Technology, Zhejiang, P.R. China “the Opening Foundation of the Environmental Engineering Key Discipline”.

References

1 P. Azadi, E. Afif, H. Foroughi, T. S. Dai, F. Azadi, R. Farnood, Appl. Catal., B., 2013, **134-135**, 265-273.

2 Y. J. Yao, R. Shen, K.G. Pennell, E. M. Suuberg, Environ. Sci. Technol., 2013, **47**, 906-913.

3 L. L. Niu, C. Xu, Y. J. Yao, K. Liu, F. X. Yang, M. L. Tang, W. P. Liu, Environ. Sci. Technol., 2013, **47**, 12140-12147.

4 Y. J. Yao, R. Shen, K.G. Pennell, E. M. Suuberg, Environ. Sci. Technol., 2013, **47**, 1425-1433.

5 A. Murray, A. Horvath, K. L. Nelson, Environ. Sci. Technol., 2008, **42**, 3163-3169.

6 J. L. Hong, J. M. Hong, M. Otaki, O. Jolliet, Waste Manage., 2009, **29**, 696-703.

7 J. Matos, M. Rosales, A. García, C. Nieto-Delgado, J. R. Rangel-Mendez, Green Chem., 2011, **13**, 3431-3439.

8 M. Balakrishnan, V. S. Batra, J. S. J. Hargreaves, I. D. Pulford, Green Chem., 2011, **13**, 16-24.

9 R. R. N. Marquesa, F. Stüber, K. M. Smith, A. Fabregat, C. Bengoa, J. Font, A. Fortuny, S. Pullket, G. D. Fowler, N. J. D. Graham, Appl. Catal., B., 2011, **101**, 306-316.

10 S. J. Yuan, X. H. Dai, Appl. Catal., B., 2014, **154-155**, 252-258.

11 D. R. Vardon, B. K. Sharma, J. Scott, G. Yu, Z. C. Wang, L. Schideman, Y. H. Zhang, T. J. Strathmann, Bioresour. Technol., 2011, **102**, 8295-8303.

12 J. A. Onwudili, P. Radhakrishnan, P. T. Williams, Environ. Technol., 2013, **33**, 529-537.

13 E. Afif, P. Azadi, R. Farnood, Appl. Catal., B., 2011, **105**, 136-143.

14 S. M. Kang, X. L. Li, J. Fan, J. Chang, Ind. Eng. Chem. Res., 2012, **51**, 9023-9031.

15 Y. J. Yao, Z. H. Yang, H. Q. Sun, S. B. Wang, Ind. Eng. Chem. Res., 2012, **51**, 14958-14965.

16 S. H. Liang, F. Teng, G. Bulgan, R. L. Zong, Y. F. Zhu, J. Phys. Chem. C., 2008, **112,** 5307-5315.

17 L. L. Xu, X. F. Li, J. Q. Ma, Y. Z. Wen, W. P. Liu, Appl. Catal., A: General, 2009, **20,** 432-437.

18 T. T. Truong, Y. Z. Liu, Y. Ren, L. Trahey, Y. G. Sun, ACS Nano. 2012, **6**, 8067-8077.

19 Y. Z. Wen, W. Q. Liu, Z. H. Fang, W. P. Liu, J. Environ. Sci., 2005, **17**, 766-769.

20 C. S. Shen, Y. Z. Wen, Z. L. Shen, J. Wu, W. P. Liu, J. Hazard. Mater., 2011, **193**, 209-215.

21 X. F. Li, X. Liu, L. L. Xu, Y. Z. Wen, J. Q. Ma, Z. C. Wu, Appl. Catal., B., 2015, **165**, 79-86.

22 Y. Z. Wen, C. S. Shen, Y. Y. Ni, S. P. Tong, F. Yu, J. Hazard. Mater., 2012, **201-202**, 162-169.

23 L. X. Hu, F. Yang, W. C. Lu, Y. Hao, H. Yuan, Appl. Catal., B., 2013, **134-135**, 7-18.

24 C. Areeprasert, P. T. Zhao, D. C. Ma, Y. F. Shen, K. Yoshikawa, Energy Fuels, 2014, **28**, 1198-1206.

25 D. P. Dubal, D. S. Dhawale, R. R. Salunkhe, C. D. Lokhande, J. Electrochem.

Soc., 2010, **157**, 812-817.

26 H. Chen, J. He, J. Phys. Chem. C., 2008, **112**, 17540-17545.

27 C. H. Kuo, C. K. Lee, Carbohydr. Polym., 2009, **77**, 41-46.

28 M. L. Chacón-Patiño, C. Blanco-Tirado, J. P. Hinestrozab, M. Y. Combariza, Green Chem., 2013, **15**, 2920-2928.

29 G. K. Parshetti, Z. Liu, A. Jain, M. P. Srinivasan, R. Balasubramanian, Fuel, 2013, **111**, 201-210.

30 N. N. Tušar, D. Maucec, M. Rangus, I. Arcon, M. Mazaj, M. Cotman, A. Pintar, V. Kaucic. Adv. Funct. Mater., 2012, **22,** 820-826.

31 Y. H. Guan, J. Ma, Y. M. Ren, Y. L. Liu, J. Y. Xiao, L. Q. Lin, C. Zhang, Water Res., 2013, **47,** 5431-5438.

32 C. S. Shen, Y. Shen, Y. Z. Wen, H. Y. Wang, W. P. Liu, Water Res., 2013, **45,** 5200-5210.

33 X. R. Xu, X. Z. Li, Sep. Purif. Technol., 2010, **72**, 105-111.

34 S. Y. Yang, P. Wang, X. Yang, L. Shan, W. Y. Zhang, X. T. Shao, R. Niu, J. Hazard. Mater., 2010, **179**, 552-558.

35 Y. R. Wang, W. Chu, J. Hazard. Mater., 2011, **186**, 1455-1461.

36 L. Zhao, Z. Z. Sun, J. Ma, H. L. Liu, J. Mol. Catal. A: Chem., 2010, **322**, 26-32.

37 F. Ji, C. L. Li, X. Y. Wei, J. Yu, Chem. Eng. J., 2013, **231**, 434-440.

38 S. N. Su, W. L. Guo, Y. Q. Leng, C. L. Yi, Z. M. Ma, J. Hazard. Mater., 2013, **244-245**, 736-742.

39 Y. J. Yao, C. Xu, J. C. Qin, F. Y. Wei, M. N. Rao, S. B. Wang, Ind. Eng. Chem.

Res., 2013, **52**, 17341-17350.

40 W. P. Liu, L. L. Xu, X. F. Li, C. S. Shen, S. Rashid, Y. Z. Wen, W. P. Liu, X. H. Wu, RSC Adv., 2015, **5,** 2449-2456.

41 U.S. Environmental Protection Agency Washington, DC, 2011. Drinking Water Standards and Health Advisories [online] Available from: http://www.epa.gov/index.html.

42 C. B. Xu, J. Lancaster, Water Res., 2008, **42,** 1571-1582.

43 M. Goto, R. Obuchi, T. Hirose, T. Sakaki, M. Shibata, Bioresour. Technol., 2004, **93**, 279-284.

44 L. M. Wang, W. P. Liu, C. X. Yang, Z. Y. Pan, J. Y. Gan, C. Xu, M. R. Zhao, D. Schlenk, Environ. Sci. Technol., 2007, **31**, 6124-6128.

45 J. Liu, Y. Yang, Y. Yang, Y. Zhang, W. P. Liu, Toxicology, 2011, **282**, 47-55.

46 Y. Yang, H. H. Ma, J. H. Zhou, J. Liu, W. P. Liu, Chemosphere, 2014, **96**, 146-154.

Table 1 Chemical compositions of AS and HCAS

	Ultimate analysis (wt%)				Molar ratio	
Samples	C	H	O	N	H/C	O./C
AS	14.75	3.27	13.34	2.13	2.66	0.68
HCAS-120	13.56	2.86	11.41	1.62	2.53	0.63
HCAS-200	9.02	1.90	7.18	0.59	2.52	0.60

HCAS-120: the anaerobic sludge (AS) was treated by hydrothermal method at 120 ºC; HCAS-200: the anaerobic sludge (AS) was treated by hydrothermal method at 200 ºC.

Table 2 Degradation efficiency of common anionic dyes

Dyes	Degradation Rate (%)	Pictures of Experiment
AR1	98.5	Control
AB25	96.9	
AB40	96.2	
AB62	99.9	
AB113	96.5	MnO_x/HCAS
AB193	97.7	
RB74	97.4	
RR11	95.4	
RR24	95.2	

The initial concentration 50 mg/L, 10 mL, T=25 ℃, pH 7.0±0.2, MnO_x/HCAS catalyst dosage 0.01 g, Oxone dosage 1.0 g/L

FIGURE CAPTIONS

Figure. 1. (a) and (b) SEM images of HCAS (anaerobic sludge treated by hydrothermal method). (c) and (d) SEM imags of MnO_x/HCAS (MnO_x-loaded HCAS through hydrothermal process).

Figure. 2. Normalized Mn K-edge XANES data of MnO_x/HCAS sample and Mn reference samples (Mn metal, MnO, Mn_3O_4, Mn_2O_3 and MnO_2).

Figure. 3. Degradation efficiency of AR 73 (Initial concentration 50 mg/L, 100 mL, T=25 ºC, pH 7.0±0.2, samples dosage 0.1 g, Oxone dosage 1.0 g/L).

Figure. 4. (a-b) Effect of inorganic salts on AR 73 degradation (Initial concentration 50 mg/L, 100 mL, T=25 ºC, pH 7.0±0.2, MnO_x/HCAS catalyst dosage 0.1 g, Oxone dosage 1.0 g/L). (c) Effect of reaction temperature on AR 73 degradation (Initial concentration 50 mg/L, 100 mL, pH 7.0±0.2, MnO_x/HCAS catalyst dosage 0.1, Oxone dosage 1.0 g/L g).

Figure. 5. (a) Degradation of AR 73 in the recycle experiment (Initial concentration 50 mg/L, 100 mL, T=25 ºC, pH 7.0±0.2, MnO_x/HCAS catalyst dosage 0.1 g, Oxone dosage 1.0 g/L). (b) Concentrations of heavy metals in MnO_x/HCAS catalyst before and after reaction, as well as leaching in the remnant solution.

Figure. 6. STXM analysis of dual-engery element distribution of heavy metals in the MnO_x/HCAS catalyst before reaction and after five recycling runs.

Figure. 7. Degradation and adsorption of AR 73 by different sludge based MnO_x (Initial concentration 50 mg/L, 10 mL, T=25 ºC, pH 7.0±0.2, Oxone dosage 1.0 g/L, catalysts dosage 0.01 g, A: anaerobic sludge obtained from brewery; B: anaerobic

sludge obtained from paper mill; C: aerobic sludge obtained from secondary treatment for urban waste water; D: anaerobic sludge obtained from pig farm; E: anaerobic sludge obtained from chemical factory; F: anaerobic sludge obtained from primary treatment for dyeing wastewater; G: anaerobic sludge obtained from secondary treatment for dyeing wastewater; H: anaerobic sludge obtained from tertiary treatment for dyeing wastewater; I: aerobic sludge obtained from secondary treatment for dyeing wastewater; J: aerobic sludge obtained from secondary treatment for textile wastewater).

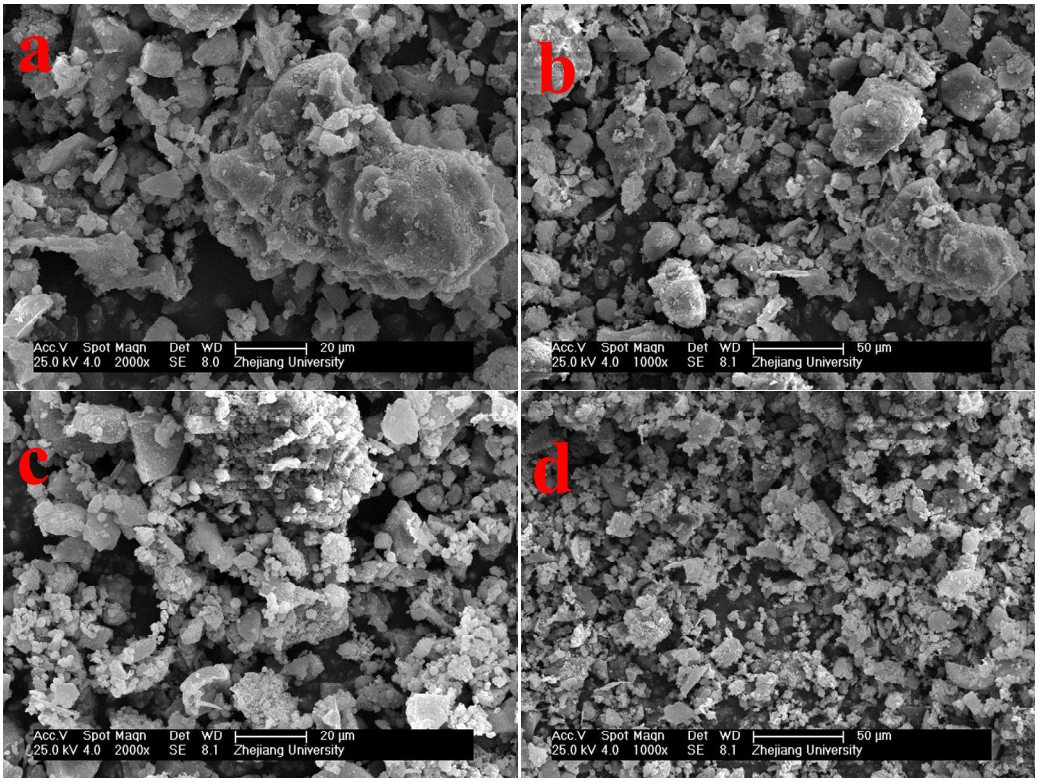

Figure. 1

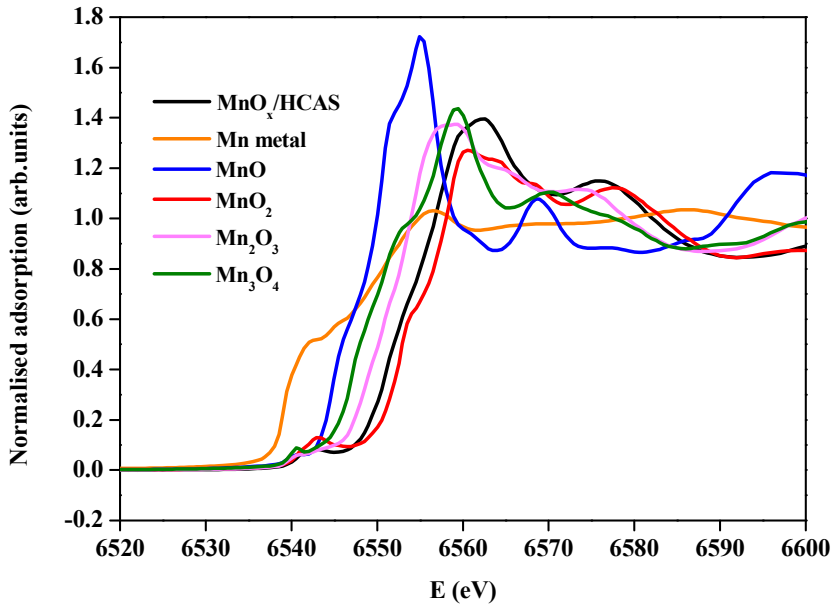

Figure. 2

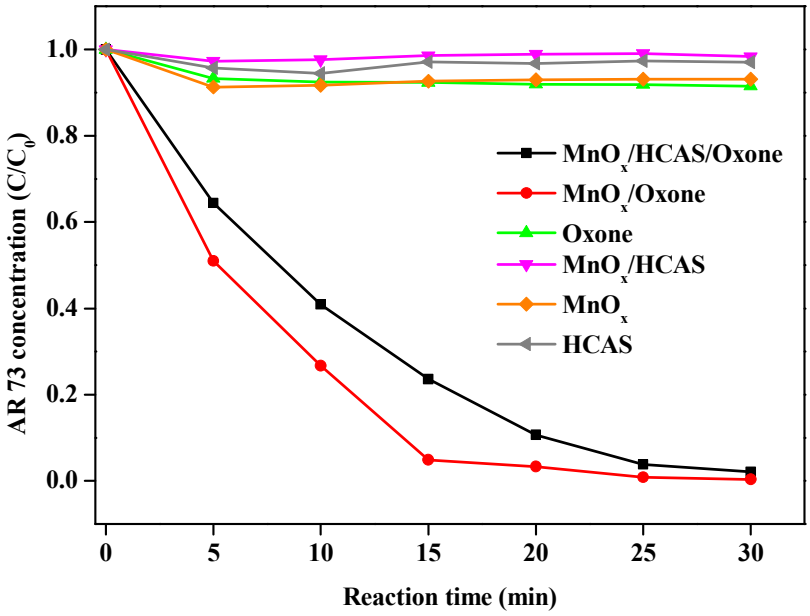

Figure. 3

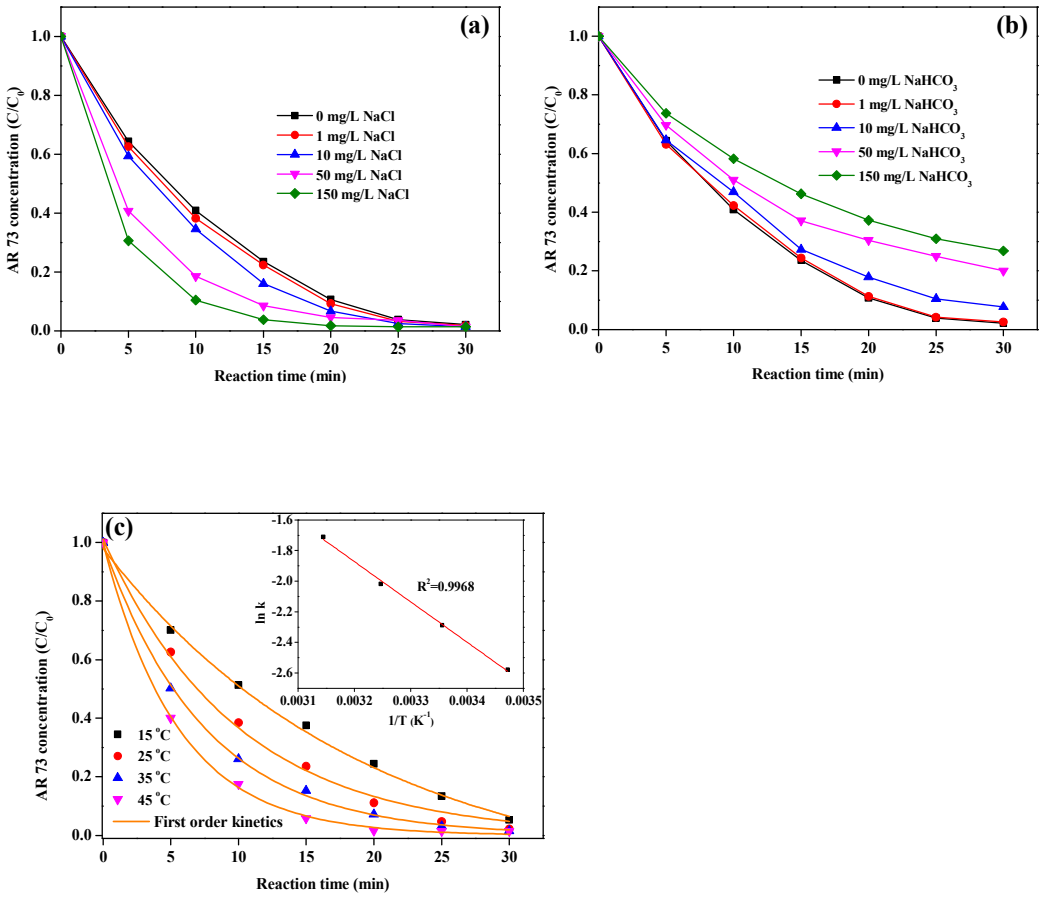

Figure. 4

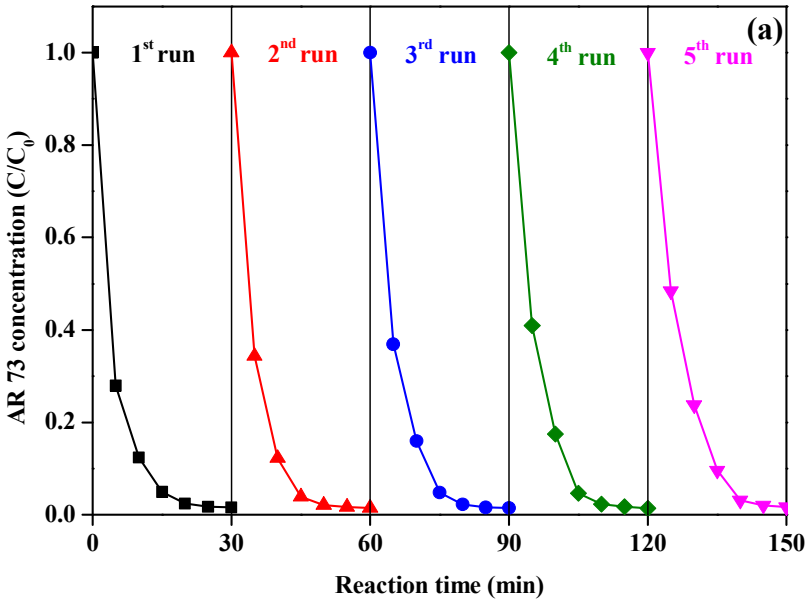

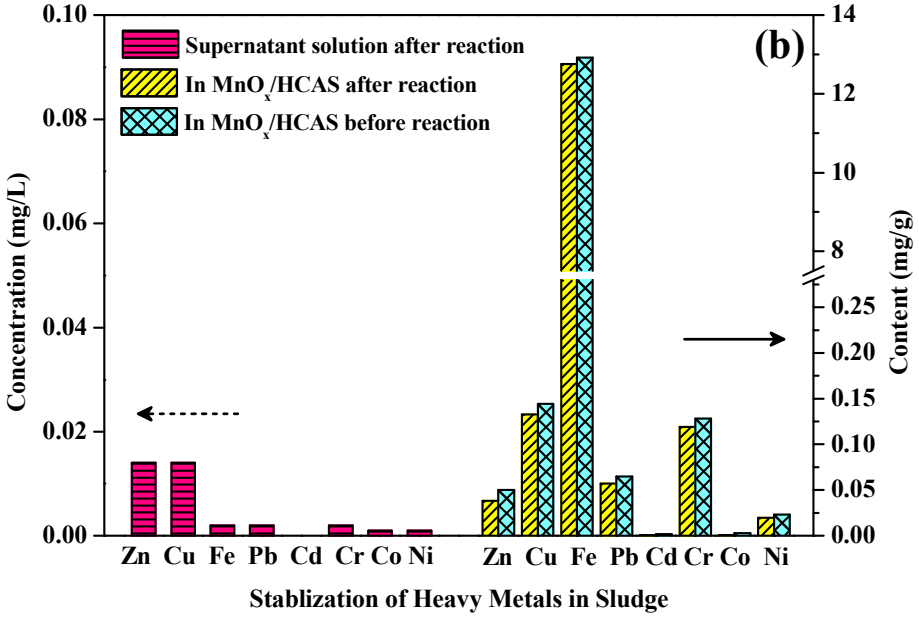

Figure. 5

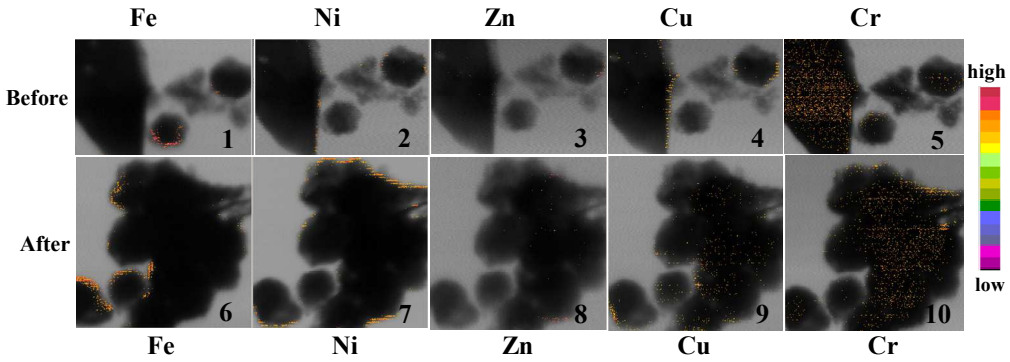

Figure. 6

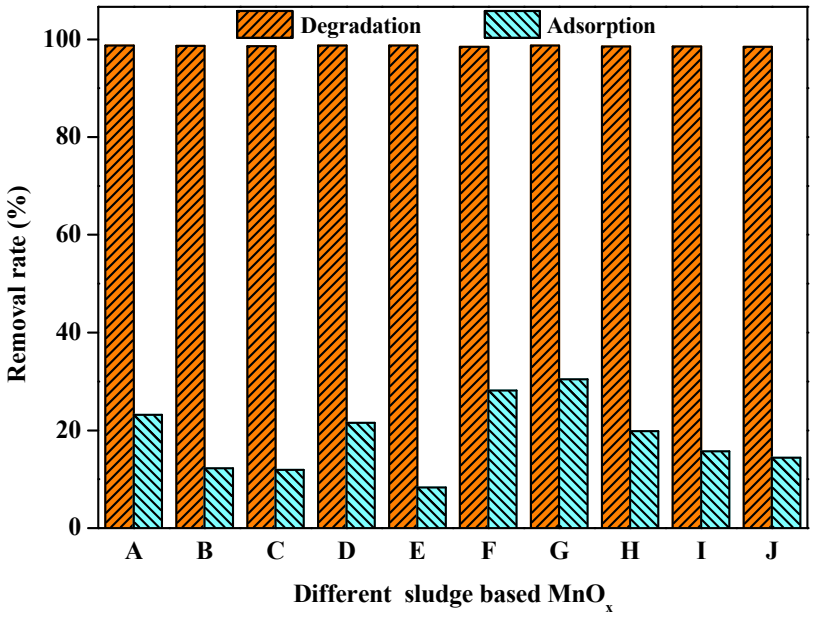

Figure. 7